horticulturae

MDPI

Article

Differentiating Leaf Structures and Physiological Responses to Freezing Stress of Mangrove *Kandelia obovata* from Different Provenances

Wenzhen Xin [1,2], Xia An [3], Huizi Liu [1], Shuangshuang Liu [1], Sheng Yang [1], Xin Wei [1], Jiali Zhao [4], Renan Lin [5], Xing Liu [1,*] and Qiuxia Chen [1,*]

1 Wenzhou Key Laboratory of Resource Plant Innovation and Utilization, Zhejiang Institute of Subtropical Crops, Zhejiang Academy of Agricultural Sciences, Wenzhou 325005, China; xinwenzhen1997@163.com (W.X.); liuhuizi1140@163.com (H.L.); liushuangshuang202@163.com (S.L.); yangsheng0072001@sina.com (S.Y.); weixindiqiu@163.com (X.W.)
2 College of Life and Environmental Sciences, Wenzhou University, Wenzhou 325000, China
3 Zhejiang Xiaoshan Institute of Cotton & Bast Fiber Crops, Zhejiang Institute of Landscape Plants and Flowers, Zhejiang Academy of Agricultural Sciences, Hangzhou 311251, China; anxia@zaas.ac.cn
4 Jilin Provincial Academy of Forestry Sciences, Changchun 130033, China; cloudie1990@sina.com
5 Yueqing Bureau of Natural Resources and Planning, Wenzhou 325600, China; linrenan308@163.com
* Correspondence: liuxingzy1989@163.com (X.L.); yzscqx@163.com (Q.C.)

Abstract: *Kandelia obovata* (Rhizophoraceae) is the most cold-tolerant mangrove species and has been widely used in coastal wetland ecological restoration due to its specific viviparous phenomenon, beautiful shape, and unique floral pattern. Due to long-term adaptation to their local environment, the phenotypic characteristics and stress resistance of widely distributed plants of the same species often differentiate across different locations. The capacity for cold resistance is closely linked to the physiological and structural characteristics of plants. Herein, we explored the temporal variations in the leaf structure and physiological status of *K. obovata* under −5.5 °C from different areas such as Jiulongjiang Estuary (JLJ, 24°25′ N), Fujian Province, and Longgang City (LG, 27°34′ N) and Jiaojiang District (JJ, 28°67′ N), Zhejiang Province. The morphological variations implied that the cold resistance of *K. obovata* obviously strengthened after the northward migration and acclimatization, in the following order: LG > JJ > JLJ. More specifically, after exposure to a sustained low temperature, the relative conductivity (REC), an index widely used to evaluate the degree of plant damage, remarkably increased from 33.62 ± 2.39 to 63.73 ± 3.81, 31.20 ± 1.63 to 49.48 ± 1.12, and 23.75 ± 0.13 to 54.24 ± 1.45 for JLJ, LG, and JJ, respectively ($p < 0.05$). Additionally, the palisade-to-spongy tissue ratio (P/I) of JLJ and JJ decreased from 0.78 ± 0.05 and 0.75 ± 0.03 to 0.5 ± 0.04 and 0.64 ± 0.02 ($p < 0.05$), whereas no significant changes were found in LG ($p > 0.05$). The SOD activity of LG significantly kept increasing, with values increased from 352.49 ± 10.38 to 477.65 ± 1.78 $U \cdot g^{-1}$, whereas no apparent changes in JLJ and JJ were observed with the sustained low temperature. The results of this study improved our understanding of the response of *K. obovata* to freezing stress, which could provide a sound theoretical foundation for cultivating cold-resistant varieties, as well as expanding mangrove plantations in higher latitudes.

Keywords: *Kandelia obovata*; low temperature; physiological responses; anatomical structure; palisade-to-spongy tissue ratio; SOD

Citation: Xin, W.; An, X.; Liu, H.; Liu, S.; Yang, S.; Wei, X.; Zhao, J.; Lin, R.; Liu, X.; Chen, Q. Differentiating Leaf Structures and Physiological Responses to Freezing Stress of Mangrove *Kandelia obovata* from Different Provenances. *Horticulturae* **2024**, *10*, 182. https://doi.org/10.3390/horticulturae10020182

Academic Editor: Aušra Brazaitytė

Received: 15 January 2024
Revised: 7 February 2024
Accepted: 14 February 2024
Published: 17 February 2024

1. Introduction

Mangroves, known as Earth's kidney, are the only woody halophytes living at the confluence of land and sea, spanning over 118 countries and territories with a total area of ~1.7 million hectares [1,2]. They serve many important ecological and commercial functions such as biodiversity maintenance, coastal erosion prevention, and carbon sequestration. It is well known that mangroves are a particularly vulnerable group of temperature-sensitive

plants, and their natural distribution in China is only from Sanya (18°12′ N), Hainan Province, to Fuding (27°20′ N), Fujian Province. With the help of global warming, mangroves could be pushed to their latitudinal limits. For example, Chen et al. [3] reported that mangroves would extend to Nanjing (32°37′ N), Jiangsu Province, if the global temperature rises by more than 4.0 °C. Consequently, many attempts have been made to transplant mangroves in higher latitudes, including Wenzhou (27°56′ N), Taizhou (28°41′ N), Zhoushan (29°93′ N), Shanghai (30°53′ N), and Qidong (31°59′ N), but the accompanying extreme-cold event could lead to physiological damage, mortality, and range contraction [4]. According to our observations, an extremely low temperature of −5.5 °C occurred in Yueqing Bay (28°20′ N) in January 2016, which caused severe damage to or even the complete loss of some introduced mangroves. Therefore, it is of great significance to characterize and understand how mangroves adapt and acclimate to this freezing temperature.

Temperature, one of the primary factors affecting plants, can induce altitudinal and latitudinal differentiation in plant populations [5,6]. It is well known that cold stress obviously changes the morphological structure and physiological and metabolic characteristics of plants, and that leaves are the most affected organ [7,8]. For example, plants growing in regions with lower temperatures often have a thicker cuticle (CT) layer, a decreased proportion of spongy tissue (ST), and an increased proportion of palisade tissue (PT) in their leaves [9]. Due to long-term adaptation to the local environment, the leaf traits of widely distributed plants of the same species often differentiate between different locations, which may be caused by phenotypic plasticity or genetic variation [10,11].

Kandelia obovata (Rhizophoraceae) is the most cold-tolerant mangrove species [12] and has been widely used in coastal wetland ecological restoration due to its specific viviparous phenomenon, beautiful shape, and unique floral pattern [13]. Recognizing the ecological and economic value of mangroves, the government of Zhejiang Province has initiated a growing series of *K. obovata* afforestation programs since the late 1950s. Nowadays, Zhejiang Province has >600 ha of mangroves in a monospecific stand of *K. obovata*, and more than 350 ha is planned to be planted within the next 5 years. Using AFLP and InDel markers, both Ruan et al. [14] and Liu et al. [11] found significant differentiation between most population pairs of *K. obovata* along the southeastern coast of China. Lu et al. [6] also observed genetic differentiation in *K. obovata* among its natural populations along the latitudinal gradient, and that the most cold-tolerant group came from the northernmost population. Notably, it is unknown whether the difference in cold resistance of artificial *K. obovata* populations is associated with their provenance differentiation.

It has been reported that Jiulongjiang Estuary (JLJ, 24°25′ N) is the distribution center of *K. obovata* in the world. The *K. obovata* located in Longgang City (LG, 27°34′ N) was recognized as cold-resistant varieties by the Forestry Department of Zhejiang Province in 2018 [15]. The Jiaojiang District (JJ, 28°67′ N) contains the northernmost artificial *K. obovata* capable of natural reproduction. In this study, we assumed that the leaf structure and physiological characteristics of *K. obovata* were genetically adapted to the coldest monthly temperature. The objective of this study was to evaluate the temporal variations in physiological status, as well as differences in leaf structure, between these three *K. obovata* provenances under a continuous low temperature of −5.5 °C. The results of this study could improve our understanding of the response and adaptability of *K. obovata* to freezing stress, which could provide a sound theoretical foundation for cultivating cold-resistant varieties, as well as expanding mangrove plantations in higher latitudes.

2. Materials and Methods

2.1. Plant Materials and Experimental Design

The *K. obovata* hypocotyls of three provenances were collected in April–May 2021 from Jiulongjiang Estuary (JLJ, 24°25′ N), Fujian Province, Longgang City (LG, 27°34′ N), Zhejiang Province, and Jiaojiang District (JJ, 28°67′ N), Zhejiang Province, respectively. The climatic characteristics of the three areas are shown in Table 1. The healthy hypocotyls were selected and soaked in a 0.5% potassium permanganate solution for 15 min. After

rinsing with water, they were put into 8 × 10 cm non-woven fabric seedling bags with mud from intertidal areas. The bottom of the hypocotyl was inserted into the soil matrix to a depth of approximately one-third of the total soil depth. Then, they were then placed in the intertidal zone of Niyu Island (24°52′ N, 121°02′ E), Dongtou District, Wenzhou City, Zhejiang Province, China, for cultivation. This area has a subtropical marine monsoon climate with an average annual temperature of 17.5 °C. The lowest temperature occurs in February, reaching −3.6 °C, while the highest temperature occurs in August, with a value of 35.7 °C. The frost-free period lasts for ~350 days per year, and the average annual rainfall is 1319.4 mm. The soil in the study area originates from modern marine and fluvial deposits (marinic aqui-orthic halosols). The soil texture is silty clay loam (USDA classification), and the basic soil physico-chemical properties were recorded as follows: pH, 8.03~8.44; salt content, 16.06~33.24 g kg^{-1}; organic matter, 14.11~35.70 g kg^{-1}; alkali-hydrolyzable N, 14.55~44.70 mg kg^{-1}; available P, 5.44~12.03 mg kg^{-1}; available potassium, 730.94~2373.88 mg kg^{-1}.

Table 1. Geographical location, climatic characteristics, and hypocotyl information of *K.obovata* from different provenances.

Provenance	Geographical Coordinates	Annual Minimum Temperature (°C)	Annual Maximum Temperature (°C)	Hypocotyl Length (cm)	Hypocotyl Ground Diameter (mm)	Hypocotyl Weight (g)
JLJ	24°25′ N, 117°55′ E	5	40	22.16 ± 0.58	11.99 ± 0.86	14.92 ± 1.19
LG	27°34′ N, 120°36′ E	−4	38	17.03 ± 0.13	9.75 ± 0.09	7.83 ± 0.12
JJ	28°67′N, 121°43′ E	−5	39	17.53 ± 0.09	9.91 ± 0.21	7.93 ± 0.15

Note: values are expressed as mean ± SD (n = 30); JLJ: Jiulongjiang Estuary, Fujian Province; LG: Longgang City, Zhejiang Province; JJ: Jiaojiang District, Zhejiang Province; the same below.

In December 2021, 100 *K. obovata* seedlings from each provenance of similar sizes were selected and transferred to plastic pots (10 cm in diameter and 11 cm in height) with tidal mud substrate and saltwater solution (5 ‰) reaching just below the base of the plants. Then, all of the seedlings were placed in a controlled climate chamber (SAFE-DG-ZJNKY-6) for low-temperature stress testing. The experimental conditions were set as follows: 8 h of short daylight, light intensity of 1000 Lx, relative humidity of 75%, and a temperature of −5.5 °C. Samples were randomly chosen and taken at 8 h, 24 h, and 48 h, respectively. More specifically, the second set of leaves below the shoot apex was collected for anatomical analysis, while the third set of leaves was used for physiological analysis. Finally, the collected leaves were cut into lengths of approximately 0.5–1 cm, taking care to avoid buds.

2.2. Determination of Leaf Anatomy

Segments of 1 cm were sequentially fixed in Carnoy's solution, dehydrated using an alcohol gradient dehydration method, embedded in paraffin, sliced using an RM2016 paraffin microtome, stained with sarranine-fast green, and sealed with neutral gum. The treated segments were randomly selected, observed, and photographed under a light microscope (HT7700, Hitachi, Ltd., Tokyo, Japan) in an upright position. The sliced images were measured using K-viewer(1.5.3.1) software [16], and parameters including leaf thickness (LT), cuticle thickness (CT), epidermis thickness (ET), hypodermis thickness (HT), palisade tissue thickness (PT), and spongy tissue thickness (ST) were obtained. The tissue looseness index (SR), tissue compactness ratio (CTR), and palisade-to-spongy tissue ratio (P/I) were calculated as follows: SR = ST/LT, CTR = PT/LT, and P/I = PT/ST.

2.3. Determination of Leaf Physiological Changes

About 0.1 g of the leaf samples was heated in boiling water for 30 min, then centrifuged at 5000× g rpm, and the soluble sugar (SS) concentration of the supernatant was measured using the anthrone colorimetric method. For the proline (Pro) detection, approximately 0.1 g of the leaf samples was homogenized in 3% aqueous sulfosalicylic acid, heated at 100 °C for 30 min, and filtered. Then, the filtrate was mixed with acid-ninhydrin and glacial

acetic acid (1:1:1, *v*/*v*/*v*) in a water bath at 100 °C for 1 h. Finally, the reaction mixture was extracted with toluene and the absorbance was determined at 520 nm [17].

The soluble protein (SP) content and the activities of superoxide dismutase (SOD), peroxidase (POD), catalase (CAT), and ascorbate peroxidase (APX) were determined according to the method of Liu et al. [4], Shi et al. [18], and Xu et al. [8]. For the SP, SOD, POD, CAT, and APX detection, approximately 0.1 g of the leaf samples was taken into a mortar, and 1 mL ice-cold sodium phosphate-buffered solution (50 mmol L^{-1}, pH 7.0) mixed with ethylenediaminetetraacetic acid (1.0 mmol L^{-1}) and 2% polyvinylpyrrolidone was added in an ice bath. Then, the homogenate was centrifuged at 5000× *g* rpm, 4 °C for 10 min, and the supernatant was collected. The SP content was measured with the Coomassie brilliant blue staining method. The SOD activity was measured following the photoreduction of nitroblue tetrazolium assay. For the determination of POD, a mixture of 50 mL of 50 mmol phosphate buffer (pH 7.8), 28 µL of guaiacol, 19 µL of 30% H_2O_2, and 200 µL of enzyme solution was reacted for 30 min, and a colorimetric assay was performed at 470 nm. For the determination of CAT, a mixture of 1 mL of 50 mmol Tris-HCl, 1.75 mL of water, and 0.05 mL of enzyme solution was reacted for 3 min, and then 0.2 mL of H_2O_2 was added to determine the absorbance value at 240 nm. For APX, a mixture of 0.65 mL of water, 0.1 mL of 50 mmol phosphate buffer (pH 7.8), 0.1 mL of 2 mmol ascorbic acid, 0.05 mL of enzyme solution, and 0.1 mL of 2 mmol H_2O_2 was used to determine the absorbance value at 290 nm.

The content of H_2O_2 was measured as follows: a 0.06 g sample was extracted with 2 mL of 5% trichloroacetic acid, and then 100 µL of 20% titanium tetrachloride, 200 µL ammonia, and 3 mL sulfuric acid were added for color development, and finally a colorimetric assay was performed at 410 nm [8]. The thiobarbituric acid (TBA) method was used to determine the malondialdehyde (MDA) level [19]. Briefly, ~0.5 g of leaf segments was placed in 5 mL 10% trichloroacetic acid and centrifuged at 5000× *g* rpm. Then, the supernatant was mixed with 2 mL of 0.67% thiobarbituric acid, heated at 100 °C for 30 min, and centrifuged at 5000× *g* rpm. The absorbance values at 450 nm, 532 nm, and 600 nm wavelengths were recorded, respectively. The MDA content was calculated based on the following formula: C (µmol L^{-1}) = 6.452 × (A_{532} − A_{600}) − 0.559 × A_{450}. The relative electrical conductivity (REC) was determined using the water bath method [20]. For example, the initial conductivity (EL1) was measured using a conductivity meter (DDSJ-319L, Lei Magneto, Shanghai, China). Then, each sample was placed in a boiling water bath for 30 min and oscillated at room temperature (150 rpm) for 10 h. The final conductivity (EL2) was measured, and the REC value was calculated as EL1/EL2 (%). The flavonoid content (Fla) was measured as follows: 20 µL of the sample, 4 µL of 10% aluminum nitrate, 4 µL of 1 M potassium acetate, and 172 µL of ethanol were mixed in the wells of a 96-well plate.

2.4. Statistical Analysis

Data are expressed as average ± standard errors of three biological replicates. A one-way analysis of variance (one-way ANOVA) was conducted for statistical analysis, followed by Duncan's test using SPSS version 21.0 (SPSS, Chicago, IL, USA). SigmaPlot version 12.5 software was used for data visualization. A significance level of $p < 0.05$ or $p < 0.01$ was applied.

3. Results

3.1. Comparison of Morphology in Different K. obovata Provenances under Freezing Stress

As shown in Figure 1, the cold injuries of *K. obovata* showed a trend of increasing with the sustained low temperature. More specifically, green spots appeared on the leaves of *K. obovata* in all provenances after 24 h of low-temperature treatment. Among them, the JLJ sample was seriously frost-damaged, with more than 50% of the leaves withering and 40% of the branches drying up, respectively. Less than 40% of the leaves and 30% of the branches were frost-damaged in the LG sample. With the continuous low temperature of 48 h, 100%, 90%, and 60% of the leaves, branches, and stems were frost-damaged in the JLJ

sample. For JJ, 85%, 65%, and 45% of the leaves, branches, and stems were frost-damaged. In the LG sample, 75% of the leaves were withered and 60% of the branches were dried up, whereas no damage was observed in the stems.

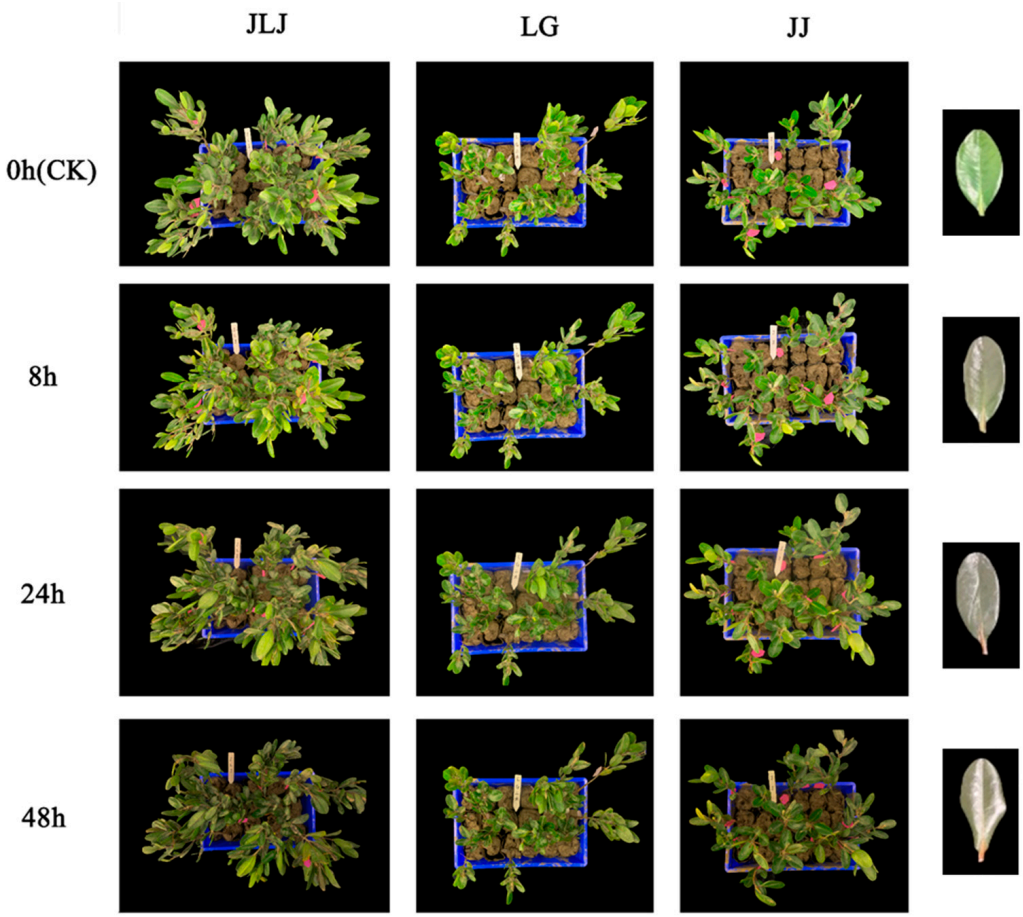

Figure 1. Morphological changes in *K. obovata* leaves from different provenances under freezing stress.

3.2. Effects of Freezing Stress on the Anatomical Structure of K. obovata Leaves

As shown in Figure 2, in the early stage of freezing stress (0~8 h), the leaf cells of *K. obovata* were injured, produced ice crystals, and gradually became thicker. With the continuous low temperature (8~48 h), the cells undergoing apoptosis within tissues gradually lost contact with their neighboring cells, especially for JLJ. As shown in Table 2, the LT values of JLJ and LG were 512.45 ± 8.80 μm and 507.94 ± 11.28 μm, respectively, significantly higher than that of JJ (439.85 ± 9.38 μm, $p < 0.05$). Similarly, all ET, PT, and ST values also exhibited the same trend: JLJ > LG > JJ. Interestingly, the CT of LG was 8.86 ± 0.31 μm, substantially higher than other two provenances (JJ, 8.12 ± 0.3 μm; JLJ, 7.23 ± 0.23 μm; $p < 0.05$). The CTR and P/I showed the following trend: JLJ > JJ > LG. For example, the P/I values for JLJ, JJ, and LG were 0.78 ± 0.05, 0.75 ± 0.03, and 0.66 ± 0.04, respectively. Overall, there are obvious differences in the leaf anatomical structures of *K. obovata* from different provenances.

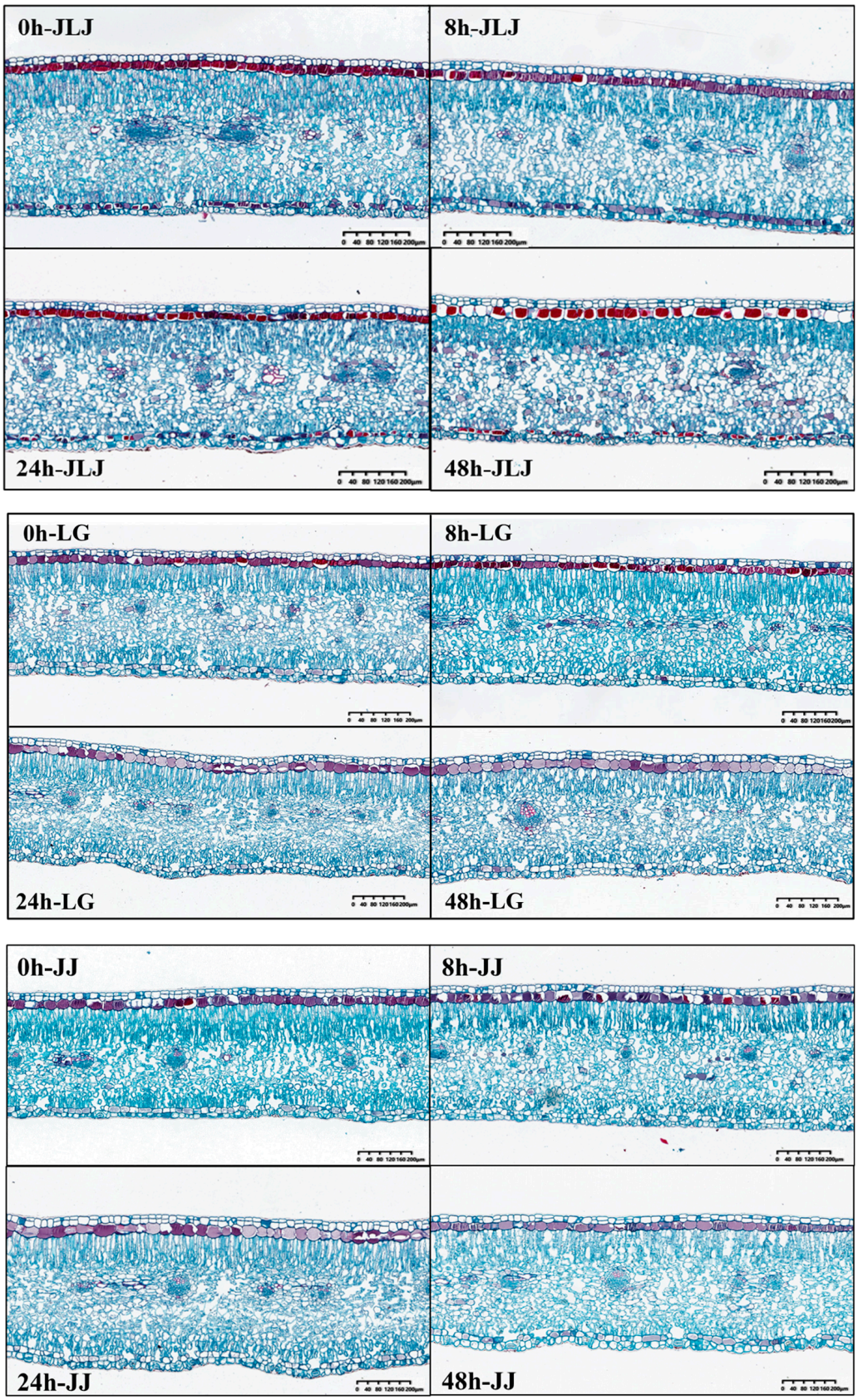

Figure 2. Varieties in the anatomic structure of *K. obovata* under low-temperature stress.

Table 2. Differences and response characteristics in the leaf structure of *K. obovata* under freezing stress.

Provenance	Item	0 h (CK)	8 h	24 h	48 h
JLJ	LT/μm	512.45 ± 8.80 c	449.90 ± 10.85 ab	437.22 ± 12.33 a	474.27 ± 13.83 b
	CT/μm	7.23 ± 0.23 a	7.78 ± 0.28 ab	8.11 ± 0.31 b	8.21 ± 0.33 b
	ET/μm	48.25 ± 1.57 b	44.82 ± 0.84 ab	47.11 ± 1.29 ab	43.73 ± 1.34 a
	HT/μm	47.9 ± 1.78 b	42.14 ± 1.24 a	42.74 ± 2.8 ab	55.63 ± 1.94 c
	PT/μm	175.46 ± 6.27 c	144.06 ± 3.56 b	139.25 ± 6.35 b	117.63 ± 5.03 a
	ST/μm	233.61 ± 10.62 bc	211.11 ± 9.74 ab	200.01 ± 7.95 a	249.07 ± 13.16 c
	CTR/%	34.36 ± 1.3 b	32.16 ± 0.79 b	31.86 ± 1.21 b	25.05 ± 1.21 a
	SR/%	45.39 ± 1.44 a	46.6 ± 1.18 a	45.73 ± 1.26 a	52.07 ± 1.49 b
	P/I	0.78 ± 0.05 b	0.7 ± 0.03 b	0.71 ± 0.05 b	0.5 ± 0.04 a
LG	LT/μm	507.94 ± 11.28 bc	510.79 ± 18.58 c	472.61 ± 11.69 ab	455.51 ± 10.20 a
	CT/μm	8.86 ± 0.31 b	8.32 ± 0.21 b	6.78 ± 0.56 a	8.54 ± 0.29 b
	ET/μm	47.69 ± 2.06 a	51.58 ± 1.71 a	47.66 ± 1.05 a	48.09 ± 1.14 a
	HT/μm	45.6 ± 2.12 a	48.98 ± 2.82 a	46.18 ± 2.26 a	49.25 ± 1.44 a
	PT/μm	157.48 ± 5.97 b	162.18 ± 6.85 b	152.07 ± 4.26 b	129.59 ± 7.44 a
	ST/μm	248.32 ± 10.09 b	239.73 ± 12.17 ab	219.93 ± 9.29 a	220.04 ± 7.05 a
	CTR/%	31.06 ± 1.13 ab	31.83 ± 0.82 b	32.29 ± 0.81 b	28.32 ± 1.36 a
	SR/%	48.7 ± 1.3 a	46.6 ± 1.06 a	46.32 ± 1.01 a	48.36 ± 1.29 a
	P/I	0.66 ± 0.04 a	0.69 ± 0.03 a	0.71 ± 0.03 a	0.6 ± 0.04 a
JJ	LT/μm	439.85 ± 9.38 a	525.99 ± 10.29 b	551.99 ± 25.18 b	448.44 ± 20.38 a
	CT/μm	8.12 ± 0.3 c	7.51 ± 0.35 bc	6.93 ± 0.2 b	5.61 ± 0.17 a
	ET/μm	45.24 ± 2.87 a	48.82 ± 5.9 ab	50 ± 1.37 b	46.87 ± 1.7 ab
	HT/μm	46.61 ± 1.38 a	45.63 ± 1.34 a	49.56 ± 1.53 a	48.39 ± 2.28 a
	PT/μm	144.57 ± 5.60 ab	159.65 ± 3.73 b	163.63 ± 8.64 b	136.64 ± 9.23 a
	ST/μm	195.32 ± 5.28 a	264.38 ± 9.98 b	281.87 ± 17.99 b	210.93 ± 10.24 a
	CTR/%	32.77 ± 0.84 b	30.46 ± 0.77 ab	29.75 ± 1.01 a	30.13 ± 0.75 a
	SR/%	44.44 ± 0.93 a	50.06 ± 1.06 b	50.63 ± 1.34 b	46.99 ± 0.61 a
	P/I	0.75 ± 0.03 b	0.62 ± 0.03 a	0.6 ± 0.03 a	0.64 ± 0.02 a

Note: LT, leaf thickness; CT, cuticle thickness; ET, epidermal thickness; HT, endodermal thickness; PT, palisade tissue thickness; ST, spongy tissue thickness; SR, tissue porosity; CTR, tissue tightness; P/I, grid-to-sea ratio; the same below. Different lowercase letters indicate significant differences in the same *K. obvata* provenance at different times during the low-temperature treatment at $p < 0.05$ according to the LSD test.

For the LT, the JLJ sample showed a trend of first decreasing and then increasing under the sustained low temperature, with the lowest value being 437.22 ± 12.33 μm at 24 h. The LT of LG significantly decreased from 507.94 ± 11.28 μm to 455.51 ± 10.20 μm ($p < 0.05$). The LT of JJ dramatically increased from 439.85 ± 9.38 μm to 525.99 ± 10.29 μm when initially exposed to freezing stress (8 h), and gradually increased with as the persisted low temperature progressed (8~24 h), and ultimately decreased to the original value (448.44 ± 20.38 μm, $p > 0.05$) at 48 h. Under freezing stress, the CT, ET, and HT values of JLJ showed an increasing–decreasing (first increasing and then decreasing) trend, respectively. There were no significant changes in the CT, ET, and HT of LG with the extension of the low-temperature stress time ($p > 0.05$). For JJ, the CT decreased, the ET increased first and then decreased, and the HT did not change significantly ($p > 0.05$). The PT and ST of all the three provenances showed a similar trend to the LT in response to the low-temperature treatment. In terms of P/I and SR, no obvious changes were found in LG under low-temperature treatment ranging from 0 to 48 h ($p > 0.05$). For JLJ and JJ, the P/I and SR exhibited the same trend, decreasing from 0.78 ± 0.05 and 0.75 ± 0.03 to 0.5 ± 0.04 and 0.64 ± 0.02, while the SR increased from 45.39 ± 1.44 and 44.44 ± 0.93 to 52.07 ± 1.49 and 50.63 ± 1.34, respectively ($p < 0.05$). To sum up, the characteristics of the response to freezing stress in the leaf structure of *K. obovata* varied significantly between provenances. As shown in Figure 3, the low-temperature stress duration was significantly negatively correlated with the PT, CTR, and P/I (Figure 3b,e,f), whereas a significant positive correlation was observed between the SR and stress duration ($p < 0.05$, Figure 3d). For LG, both PT and P/I were significantly negatively correlated with the stress duration ($p < 0.05$, Figure 3b,f).

For JJ, only the CT was obviously negatively correlated with the stress duration ($p < 0.05$, Figure 3a).

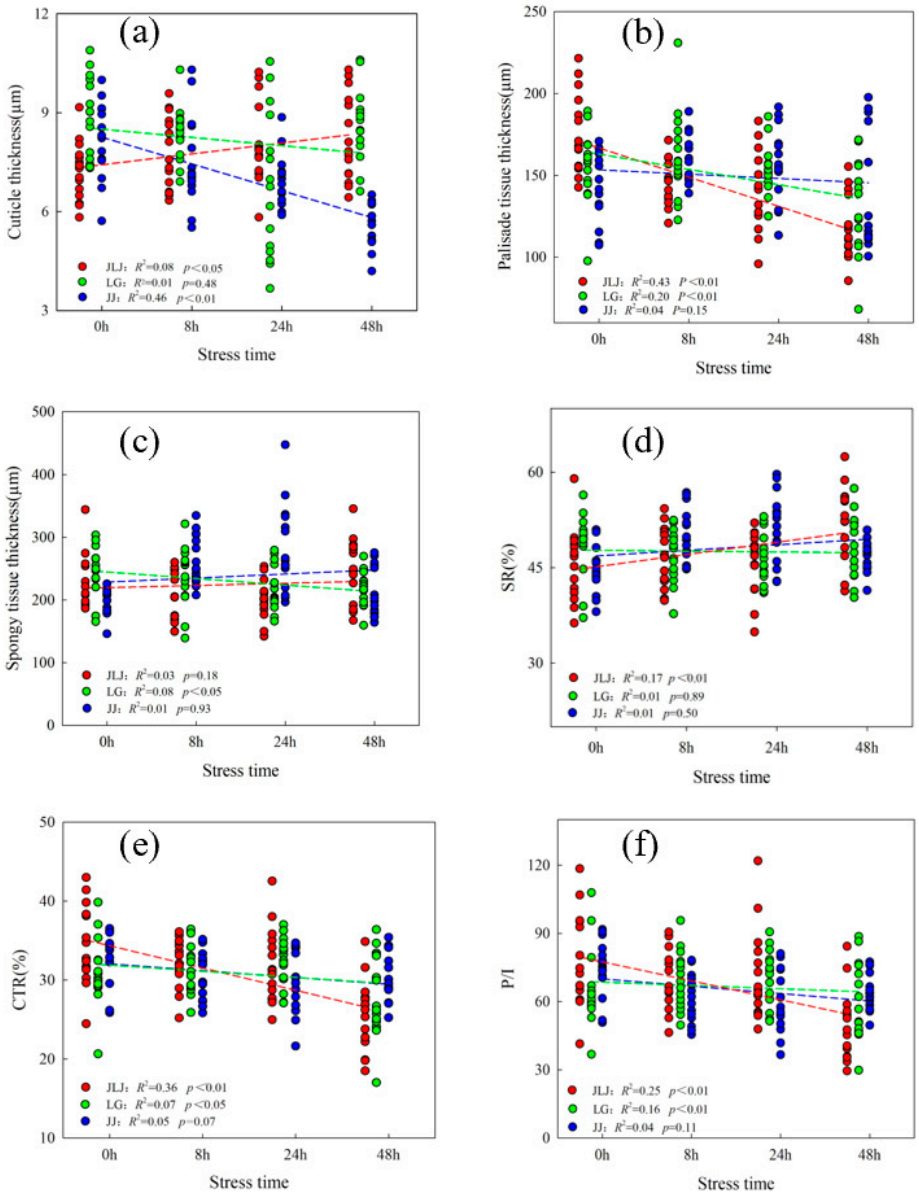

Figure 3. Correlation between cuicle thickness (**a**), palisade tissue thickness (**b**), spongy tissue thickness (**c**), tissue looseness index (**d**), tissue compactness ratio (**e**) and palisade-to-spongy tissue ratio (**f**) of the leaves and the duration of the low-temperature stress. The dashed line shows the trend of correlation between each indicator and stress duration.

3.3. The Physiological Response of K. obovata to Freezing Stress

To study the relationships between physiological status and cold tolerance in *K. obovata*, it is imperative to study a variety of osmotic adjustment substances. As shown in Figure 4, only the SS of JLJ obviously increased from 13.42 ± 0.28 to 15.78 ± 0.48 mg·g^{-1} when initially facing the freezing stress (0~8 h), which then returned to the original value at 24 h ($p > 0.05$, Figure 4b). Meanwhile, no significantly changes were observed in the SP and Pro contents of JLJ during the freezing stress period ($p > 0.05$, Figure 4a,c). For LG, the contents of SP and SS obviously increased from 51.19 ± 0.80 to 57.92 ± 2.04 mg·g^{-1} and 17.69 ± 0.22 to 18.99 ± 0.45 mg·g^{-1} (0~8 h), respectively, and then maintained a relatively stable level (8~24 h), whereas no obvious change was observed in the Pro content

(Figure 4a–c). For JJ, there were significantly changes in the SP, SS, and Pro contents between 0 and 8 h ($p > 0.05$, Figure 4a–c). From 8 to 24 h, the SP, SS, and Pro increased from 42.89 ± 1.04 to 67.68 ± 1.54 mg·g^{-1}, 18.42 ± 0.31 to 21.74 ± 0.23 mg·g^{-1}, and 36.10 ± 0.77 to 43.31 ± 0.86 μg·g^{-1}, respectively.

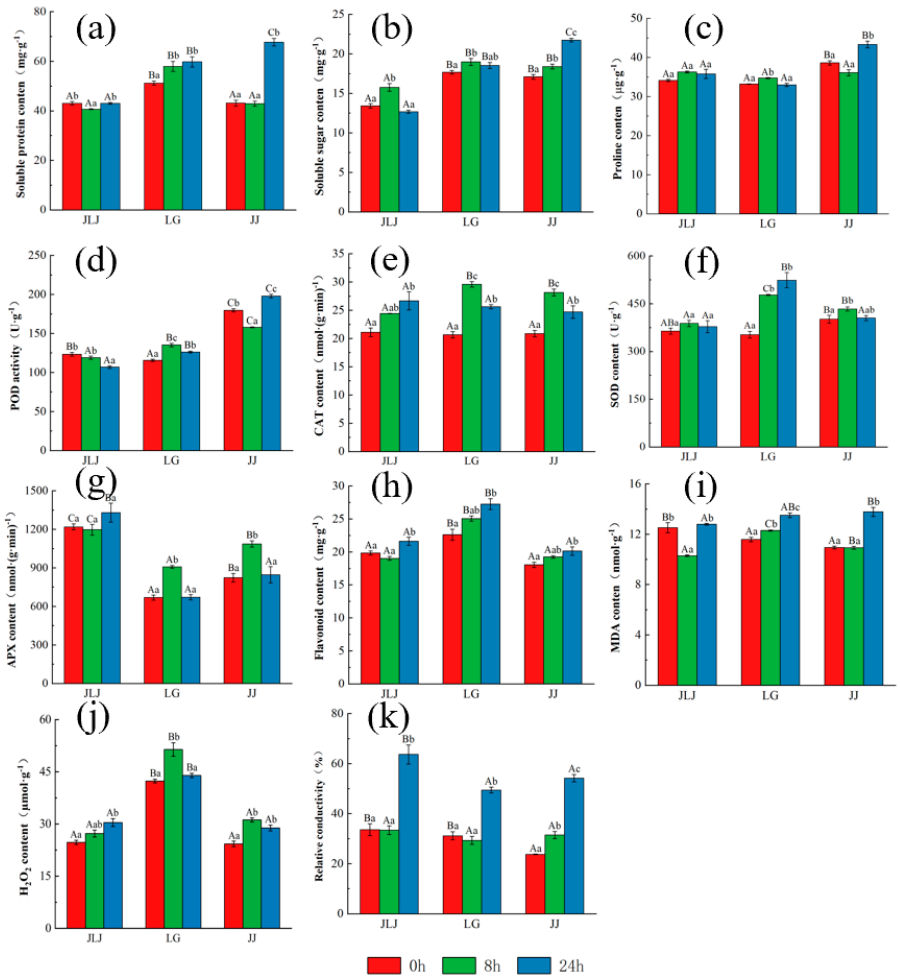

Figure 4. Changes in physiological characteristics of *K. obovata* under prolonged low−temperature treatment. (**a**) SP, soluble protein; (**b**) SS, soluble sugar; (**c**) Pro, proline; (**d**) POD, peroxidase; (**e**) CAT, catalase (**f**) SOD, superoxide dismutase; (**g**) APX, ascorbate peroxidase; (**h**) Fla, flavonoid; (**i**) MDA, malondialdehyde; (**j**) H_2O_2, hydrogen peroxide; (**k**) REC, relative conductivity. Bars and error bars indicate the mean ± standard deviation from three biological replicates. Different capital letters indicate significant differences between different *K. obovata* provenances at the same time points of the low−temperature treatment, and different lowercase letters indicate significant differences of the same *K. obovata* provenance at different time points of the low−temperature treatment at $p < 0.05$ according to the LSD test.

For JLJ, the H_2O_2 content positively increased with the sustained low temperature, with the values going from 24.73 ± 0.61 to 30.41 ± 1.12 μmol·g^{-1}. The changing trend of the H_2O_2 content in LG and JJ first increased and then decreased, reaching a peak at 8 h. Notably, only LG returned to the original value at 24 h (42.34 ± 0.54 vs. 43.95 ± 0.61, $p > 0.05$), implying the ability of *K. obovata* to remove H_2O_2 is ranked in the following order: LG > JJ > JLJ (Figure 4j). For SOD activity, there were no apparent changes induced by the sustained low temperature in JLJ and JJ. For LG, the SOD activity significantly increased from 352.49 ± 10.38 to 477.65 ± 1.78 U·g^{-1} (Figure 4f). The CAT activity of JLJ, LG, and JJ dramatically increased from 21.11 ± 0.77 to 26.70 ± 1.60 nmol·(g·min)$^{-1}$, 20.68 ± 0.56 to 29.60 ± 0.49 nmol·(g·min)$^{-1}$, and 20.88 ± 0.57 to 28.16 ± 0.61 nmol·(g·min)$^{-1}$ in the early

stage of freezing stress, and then decreased in LG and JJ, but kept increasing in JLJ (Figure 4e). When exposed to the low temperature, the POD activity decreased from 123.54 ± 2.26 to 106.94 ± 1.53 U·g^{-1} in JLJ, but increased from 115.63 ± 1.55 to 135.36 ± 2.17 U·g^{-1} in LG (Figure 4d). The APX activity of LG and JJ obviously increased from 669.31 ± 19.77 to 909.25 ± 10.47 nmol·(g·min)$^{-1}$ and 824.11 ± 33.68 to 1087.28 ± 24.39 nmol·(g·min)$^{-1}$ at 8 h, respectively, and subsequently returned to original values at 24 h. The APX activity of JLJ changed slightly between 0 and 8 h (1220.04 ± 22.80 nmol·(g·min)$^{-1}$ vs. 1197.84 ± 41.68 nmol·(g·min)$^{-1}$, $p > 0.05$), and peaked with a value of 1331.43 ± 74.18 nmol·(g·min)$^{-1}$ at 24 h (Figure 4g). The MDA contents, an indicator of damage to plant cells under stress, obviously increased from 11.59 ± 0.17 to 13.52 ± 0.18 nmol·g^{-1} and from 10.95 ± 0.11 to 13.79 ± 0.36 nmol·g^{-1} in LG and JJ, respectively. Notably, the MDA of JLJ remarkably decreased at 8 h, and then returned to the original value at 24 h (12.53 ± 0.40 nmol·g^{-1} vs. 12.80 ± 0.07 nmol·g^{-1}, $p > 0.05$, Figure 4i). The REC, another index widely used to evaluate the degree of plant damage, remarkably increased from 33.62 ± 2.39 to 63.73 ± 3.81, from 31.20 ± 1.63 to 49.48 ± 1.12, and from 23.75 ± 0.13 to 54.24 ± 1.45 for JLJ, LG, and JJ, respectively ($p < 0.05$, Figure 4k), which is consistent with the results of our analysis of morphological changes (Figure 1). Moreover, the Fla content of all three provenances significantly increased when exposing to freezing stress, especially for the LG sample (Figure 4h).

3.4. Principal Component Analysis and Membership Function Analysis of K. obovata from Different Provenances

A principal component analysis (PCA) was adopted to evaluate the contribution of the main indices to the cold resistance of *K. obovata*. The principal components 1 (PC1) and 2 (PC2) contributed 42.9% and 16.4%, respectively, with a cumulative variance contribution of 59.3%. The Fla and SOD were the closest physiological indicators to the LG clustered samples, deeming them essential factors for LG (Figure 5). As it is difficult to accurately reflect the cold resistance of plants using a single index, a comprehensive evaluation of cold resistance by combining several main physiological and biochemical indices will increase the accuracy of the results. Owing to the different units and properties of each index, the membership function method was used to evaluate these 20 indicators of leaf structure and physiological characteristics comprehensively, and consequently, an average value was obtained to evaluate the cold resistance of *K. obovata*. The greater the average membership value, the stronger the cold resistance of the sample from that provenance, and vice versa. As shown in Table 3, the average membership function values of JLJ, LG, and JJ were 0.338, 0.496, and 0.458, respectively, indicating that LG had the strongest cold resistance among the three provenances.

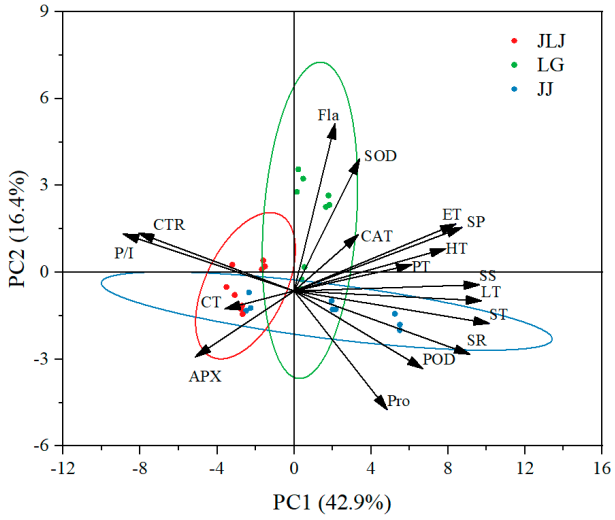

Figure 5. Principal component analysis of leaf−related indices under low−temperature stress. The circles (red, blue, green) represent how similar the samples within the group (JLJ, JJ, LG) are.

Table 3. Analysis of membership function values of *K. obovata* seedlings from different provenances under low−temperature stress.

Membership Function Value	Provenance		
	JLJ	**LG**	**JJ**
LT	0.255	0.522	0.599
CT	0.446	0.580	0.354
ET	0.282	0.615	0.472
HT	0.286	0.644	0.690
PT	0.378	0.497	0.461
ST	0.226	0.470	0.599
SR	0.237	0.447	0.636
CTR	0.666	0.435	0.285
P/I	0.758	0.508	0.357
SP	0.059	0.578	0.390
SS	0.141	0.632	0.707
Pro	0.235	0.065	0.616
MDA	0.452	0.622	0.456
H_2O_2	0.117	0.797	0.141
REC	0.496	0.323	0.319
POD	0.106	0.207	0.787
CAT	0.382	0.519	0.437
SOD	0.140	0.577	0.354
APX	0.877	0.122	0.378
Fla	0.231	0.754	0.119
Mean value	0.338	0.496	0.458
Order of stress resistance	3	1	2

4. Discussion

K. obovata is an excellent coastal wetland landscape tree due to its specific viviparous phenomena, beautiful shape, and unique floral pattern, while its northern boundary of artificial cultivation has not yet broken through Yueqing Bay (28°20′ N). This study revealed the temporal variations in the physiological status, as well as differences in the leaf structure, of *K. obovata* from three provenances with different degrees of cold resistance under a continuous low temperature of −5.5 °C. The results of this study could deepen our understanding of the leaf structure and physiological characteristics of *K. obovata* after the northward migration and acclimatization, which could provide a sound theoretical foundation for cultivating cold−resistant varieties, and consequently expanding mangrove plantations in higher latitudes.

4.1. Differential Anatomical Variations in the Leaf Structure of K. obovata from Different Provenances and Their Responses to Freezing Stress

A plant's ability to respond and adapt to environmental changes is primarily based on changes in the anatomy of its leaves [21,22]. The SR, combined with differences in the LT, PT, and ST, is often used to assess the cold tolerance of plants [23]. As shown in Figure 3, no significant correlation was found between the SR and low-temperature time for LG and JJ ($p > 0.05$), while the SR of JLJ progressively increased with increases in the stress duration ($p < 0.01$), indicating that low-latitude *K. obovata* might suffer the most severe frost damage with obvious anatomical variations (Figure 2). Maintaining photosynthesis is of essential importance for plants to survive under low temperatures. Among their various anatomical characteristics, the P/I is positively correlated with the net photosynthetic rate [24,25]. The PT and ST are increased under low temperatures, which facilitates the rapid transfer of metabolites among mesophyll cells, the consequence of which is a high photosynthetic rate [26]. Consistently, the P/I of LG was also significantly positively related with the stress duration ($p < 0.05$, Figure 2). Notably, a remarkably negative correlation was observed between the P/I and stress time ($p < 0.05$, Figure 3), implying that the leaves of JLJ might

be severely damaged, as noted in the leaf morphological observation in Figure 1. The membership function evaluation further demonstrated that the cold resistance of *K. obovata* from different provenances can be ranked in the following order: LG > JJ > JLJ. Moreover, the CT is often positively related to the cold resistance of plants [27,28]. Luis et al. [29] found that a larger CT in African oil palms (*Elaeis guineensis*) reduced the exclusion of nutrients and other substances required for the early development of pathogens, thus improving their environmental adaptability. In our study, the CTs of LG and JJ were substantially thicker than JLJ, implying that a larger leaf CT might be an adaptation of *K. obovata* to the low-temperature environment in the high latitude. Thus, improving the freezing tolerance of *K. obovata* via engineering CT synthesis is an existing possibility and should be explored more extensively. Generally, we concluded that P/I and CT could be applied to assess the cold resistance of *K. obovata*.

4.2. Temporal Variations in the Physiological Status of K. obovata from Different Provenances under Cold Stress

Botanical species have evolved several physiological and molecular adaptations, such as osmolyte accumulation, to cope with cold stress [30]. Osmotic regulators can regulate the concentration of cellular fluids, reduce the osmotic potential inside and outside the cell, and prevent water loss. The SS and SP are the main compatible solutes, and have an obviously positive correlation with the cold resistance of *K. obovata*, especially in LG and JJ (Figure 4a,b). In our study, cold stress resulted in a 13.15~57.80% increase in SP, significantly higher that seen in the SS (7.34~18.02%), implying that SP might play a more important role than SS in enhancing tolerance to freezing stress. To respond and adapt to cold stress, plants synthesize many water-soluble proteins, including antioxidative enzymes, heat-shock proteins, chaperones, and late embryogenesis abundant proteins [31]. Consistent with our findings, a previous study by Fei et al. [32] reported that while the SS maintained a relatively stable level, the SP of *K. obovata* increased gradually as time extended and then reached a peak at 12 h. Peng et al. [33] speculated that the higher increases in SP observed in *K. obovata* (43.0%) and *Aegiceras corniculatum* (44.1%) may partly account for their higher cold resistance compared to *Avicennia marina* (31%). Provart et al. [34] also found ~8000 genes involved in protein biosynthesis responding to low-temperature stress in Arabidopsis. The contents of SS and SP in JLJ exhibited a decreasing trend after 24 h of −5.5 °C exposure, indicating that this low temperature severely led to metabolism disorder in JLJ. Liu et al. [4] also observed that SS and SP exhibited a remarkably decreased tendency when initially responding to a low temperature of −4.1 °C under natural frosty conditions.

Membranes are a primary site of cold-induced injury, whose stability is considered to be a reliable indicator of cellular damage. Low temperatures can increase membrane permeability, leading to the leakage of internal solutes, decreased osmotic potential, and finally causing cell death due to water loss in severe cases. As shown in Figure 4i, the MDA, the final product of membrane peroxidation, significantly increased in the JJ and LG samples under freezing stress. However, the MDA of JLJ obviously decreased at 8 h, and then returned to its original value at 24 h, suggesting that −5.5 °C might exceed the tolerance threshold of JLJ, as it severely destroyed the membrane, and consequently influenced the detection outcomes. When plants sense low temperatures, membrane permeability increases, electrolyte exosmosis occurs, and REC increases. The REC in our study exhibited an increasing range in the following order: JLJ > JJ > LG, implying that the cold resistance of *K. obovata* strengthened after the northward migration and acclimatization. Therefore, it can be reported that the REC was a better measure as a cold resistance index for *K. obovata* (Figure 4k).

Low temperatures cause damage primarily through producing a large number of reactive oxygen species (ROS), leading to lipid peroxidation, protein degradation, and enzyme inactivation [30]. As the first line of a plant's enzymatic defense system, SOD acts as a primary defense against ROS by converting superoxide anion radicals (O_2^-) into molecular oxygen and H_2O_2. The activity of SOD remarkably increased under freezing

stress, and the largest increase was observed in the LG sample (Figure 4f). Consistently, the H_2O_2 content increased following the same order: LG > JJ > JLJ (Figure 4j), indicating that the SOD activity played a vital role in scavenging ROS. It has been reported that H_2O_2 is crucial for signaling molecules that regulate plant cold tolerance [35]. Orabi et al. [36] also found that H_2O_2 can stimulate the antioxidant system and consequently enhance tolerance to cold stress. POD and CAT mainly play the role of enzymatic degradation of H_2O_2 to avoid peroxidation of the cell membrane. The CAT activity of all three provenances dramatically increased, and then kept increasing in JLJ, but gradually decreased in LG and JJ, and then returned to original values (Figure 4e,g). Additionally, the POD activity showed the oppositive trend, decreasing in JLJ but increasing in LG and JJ when exposed to freezing stress (Figure 4d). Interestingly, obvious reductions in H_2O_2 content were observed in LG and JJ, whereas the H_2O_2 content of JLJ continued to increase as the sustained low-temperature treatment progressed. Therefore, we speculated that the ability of *K. obovata* to scavenge ROS was improved after the northward acclimation partly through regulating POD activity. The Fla content of all three provenances also remarkably increased when exposed to freezing stress, especially for the LG sample (Figure 4h). Both Korn et al. [37] and Schulz et al. [38] found that the content of Fla is positively correlated with plant freezing tolerance after cold acclimation. Therefore, we speculated that the Fla content might partly account for the strongest cold resistance of LG. To date, how the Fla content affects the cold resistance of the mangrove plant is not fully understood, and thus the role of the Fla content for *K. obovata* at low temperatures requires further investigation.

5. Conclusions

To the best of our knowledge, this is by far the northernmost artificial *K. obovata* and lowest-temperature (−5.5 °C) study on mangrove cold resistance. After the northward migration and acclimatization, the resistance of *K. obovata* to low temperatures strengthened. Notably, −5.5 °C might exceed the tolerance threshold of JLJ, with severe damage to the membrane of *K. obovata*, and thus REC might be better than MDA as a cold resistance index for future mangrove research. After northward acclimatization, the CT of the leaves became thickened and the ability to scavenge ROS improved, primarily through regulating SOD and POD activity, especially for LG. The SP might play a more important role than SS in enhancing tolerance to freezing stress. Moreover, mechanisms related to the Fla content should be further studied, which might account for the highest cold resistance of LG. Overall, it seems likely that the trend LG > JJ > JLJ exhibited by the CT, SP, SOD, and REC values reveal the levels of freezing tolerance among the three biotypes. The findings presented here could provide a sound theoretical foundation and guidance for cultivating cold-resistant varieties and aiding in expanding mangrove plantations in higher latitudes.

Author Contributions: Conceptualization, X.L. and Q.C.; methodology, W.X.; software, S.L. and X.W.; validation, S.Y., J.Z. and R.L.; formal analysis, S.L. and W.X.; investigation, W.X.; resources, X.A. and H.L.; data curation, X.W.; writing—original draft preparation, W.X. and X.L.; writing—review and editing, X.A., X.L. and Q.C.; visualization, W.X.; supervision, X.L.; project administration, X.L.; funding acquisition, Q.C. All authors have read and agreed to the published version of the manuscript.

Funding: This study was supported by the People's Government of Zhejiang Province and the Chinese Academy of Forestry (No. 2022SY08), and the Key Scientific and Technological Grant of Zhejiang for Breeding New Agricultural Varieties (No. 2021C02070-6).

Data Availability Statement: Data are contained within the article.

Acknowledgments: We would like to thank the Vegetable Institute of Zhejiang Academy of Agricultural Sciences for providing the low-temperature culture room for this study.

Conflicts of Interest: The authors declare no conflicts of interest.

References

1. Wang, Y.S.; Gu, J.D. Ecological responses, adaptation and mechanisms of mangrove wetland ecosystem to global climate change and anthropogenic activities. *Int. Biodeterior. Biodegrad.* **2021**, *162*, 105248. [CrossRef]
2. Kathiresan, K. *Mangroves: Types and Importance*, 1st ed.; Mangroves: Ecology, Biodiversity and Management; Springer: Singapore, 2021; pp. 1–31.
3. Chen, Q.X.; Zheng, J.; Wang, J.W. *Artifcial Mangrove in Zhejiang, Province*, 5th ed.; China Forestry Publishing House: Beijing, China, 2015; pp. 105–128.
4. Liu, X.; Lu, X.; Yang, S.; Liu, Y.; Wang, W.; Wei, X.; Ji, H.; Zhang, B.; Xin, W.; Wen, J.; et al. Role of exogenous abscisic acid in freezing tolerance of mangrove *Kandelia obovata* under natural frost condition at near 32°N. *BMC Plant Biol.* **2022**, *22*, 593. [CrossRef]
5. Halbritter, A.H.; Fior, S.; Keller, I.; Billeter, R.; Edwards, P.J.; Holderegger, R.; Karrenberg, S.; Pluess, A.R.; Widmer, A.; Alexander, J.A. Trait differentiation and adaptation of plants along elevation gradients. *J. Evol. Biol.* **2018**, *31*, 784–800. [CrossRef]
6. Lu, W.X.; Zhang, B.H.; Zhang, Y.Y.; Yang, S.C. Differentiation of cold tolerance in an artificial population of a mangrove species, *Kandelia obovata*, is associated with geographic origins. *Front. Plant Sci.* **2022**, *12*, 695746. [CrossRef] [PubMed]
7. Ni, X.; Sun, L.; Cai, Q.; Ma, S.; Feng, Y.; Sun, Y.; An, L.; Ji, C. Variation and determinants of leaf anatomical traits from boreal to tropical forests in eastern China. *Ecol. Indic.* **2022**, *140*, 108992. [CrossRef]
8. Xu, G.; He, M.; Zhao, D.; Lyu, D.; Qin, S. Physiological and structural changes in apple tree branches of different varieties during dormancy. *Horticulturae* **2023**, *9*, 947. [CrossRef]
9. Domínguez, E.; Cuartero, J.; Heredia, A. An overview on plant cuticle biomechanics. *Plant Sci.* **2011**, *181*, 77–84. [CrossRef]
10. Ramírez-Valiente, J.A.; Sánchez-Gómez, D.; Aranda, I.; Valladares, F. Phenotypic plasticity and local adaptation in leaf ecophysiological traits of 13 contrasting cork oak populations under different water availabilities. *Tree Physiol.* **2010**, *30*, 618–627. [CrossRef]
11. Pritzkow, C.; Williamson, V.; Szota, C.; Trouvé, R.; Arndt, S.K. Phenotypic plasticity and genetic adaptation of functional traits influences intra-specific variation in hydraulic efficiency and safety. *Tree Physiol.* **2020**, *40*, 215–229. [CrossRef] [PubMed]
12. Liu, X.; Liu, Y.; Yang, S.; Wang, J.; Lu, X.; Wei, X.; Wang, W.; Wang, J.; Chen, Q. Development and characterization of 29 InDel markers from the mangrove *Kandelia obovata* genome using a resequencing dataset. *Conserv. Genet. Resour.* **2022**, *14*, 263–266. [CrossRef]
13. Hu, M.J.; Sun, W.H.; Tsai, W.C.; Xiang, S.; Lai, X.K.; Chen, D.Q.; Liu, X.D.; Wang, Y.F.; Le, Y.X.; Chen, S.M.; et al. Chromosome-scale assembly of the *Kandelia obovata* genome. *Hortic. Res.* **2020**, *7*, 75. [CrossRef] [PubMed]
14. Ruan, Y.; Huang, B.; Lai, S.; Wan, Y.; Li, J.; Huang, S.; Liao, P. Population genetic structure, local adaptation, and conservation genetics of *Kandelia obovata*. *Tree Genet. Genomes* **2013**, *9*, 913–925. [CrossRef]
15. Chen, Q.; Zheng, J.; Zhou, W.; Wang, J.; Yang, S.; Li, X.; Lu, X.; Liu, X. A new *Kandelia obovata* cultivar 'Longgang'. *Acta Hortic. Sin.* **2019**, *46*, 2927–2928.
16. Hu, Y.; Yang, L.; Gao, C.; Liao, D.; Long, L.; Qiu, J.; Wei, H.; Deng, Q.; Zhou, Y. A comparative study on the leaf anatomical structure of Camellia oleifera in a low-hot valley area in Guizhou Province, China. *PLoS ONE* **2022**, *17*, e0262509. [CrossRef] [PubMed]
17. Liu, X.M.; Xu, Q.L.; Li, Q.; Zhang, H.; Xiao, J. Physiological responses of the two blueberry cultivars to inoculation with an arbuscular mycorrhizal fungus under low-temperature stress. *J. Plant Nutr.* **2017**, *40*, 2562–2570. [CrossRef]
18. Shi, L.; Dong, X.; Fu, H.; Chai, X.; Bao, S.; Ren, Y.; Hu, K.; Li, Q.; Chen, Z. Differences in physiological characteristics of green prickly ash germplasm resources in response to low-temperature Stress. *Horticulturae* **2023**, *9*, 1242. [CrossRef]
19. Jakhar, S.; Mukherjee, D. Chloroplast pigments, proteins, lipid peroxidation and activities of antioxidative enzymes during maturation and senescence of leaves and reproductive organs of *Cajanus cajan* L. *Physiol. Mol. Biol. Plants* **2014**, *20*, 171–180. [CrossRef] [PubMed]
20. Kim, M.; Moon, Y.E.; Han, S.G.; Yun, S.K.; Joa, J.H.; Park, J.S. Impact of cold stress on physiological responses and fruit quality of shiranuhi mandarin in response to cold conditions. *Horticulturae* **2023**, *9*, 906. [CrossRef]
21. Schreiber, S.G.; Hamann, A.; Hacke, U.G.; Thomas, B.R. Sixteen years of winter stress: An assessment of cold hardiness, growth performance and survival of hybrid poplar clones at a boreal planting site. *Plant Cell Environ.* **2013**, *36*, 419–428. [CrossRef]
22. Kaur, R.; Kaur, N.; Singh, H. Pericarp and pedicel anatomy in relation to fruit cracking in lemon (*Citrus limon* L. Burm.). *Sci. Hortic.* **2019**, *246*, 462–468. [CrossRef]
23. Cao, H.; Huang, H.; Lei, X.; Zhang, D.; Zhang, R. Difference of the leaf anatomical structure of coconut varieties under low temperature treatments. *Chin. J. Trop. Crops* **2014**, *35*, 2420–2425.
24. Duan, W.J.; Shen, Y.F.; Cao, Z.H.; Shu, Q.L.; Hu, J.J.; Li, C.S. Effect of foliar fertilizer on leaf anatomy structure and photosynthetic characteristics of Camellia oleifera container seedlings. *J. Northwest A F Univ.* **2015**, *43*, 92–97.
25. Liao, W.T.; Wang, R.H.; Zhong, F.X.; Li, T.; Chen, C.X. Comparison of photosynthetic and leaf anatomical characteristics of five excellent Camellia oleifera clones. *Non-Wood For. Res.* **2015**, *33*, 56–61.
26. Zhang, Y.; Chen, C.; Jin, Z.; Yang, Z.; Li, Y. Leaf anatomy, photosynthesis, and chloroplast ultrastructure of *heptacodium miconioides* seedlings reveal adaptation to light environment. *Environ. Exp. Bot.* **2022**, *195*, 104780. [CrossRef]
27. Domínguez, J.A.; Heredia-Guerrero, A.A. The biophysical design of plant cuticles: An overview. *New Phytol.* **2011**, *189*, 938–949. [CrossRef] [PubMed]

28. Matas, A.J.; López-Casado, G.; Cuartero, J.; Heredia, A. Relative humidity and temperature modify the mechanical properties of isolated tomato fruit cuticles. *Am. J. Bot.* **2005**, *92*, 462–468. [CrossRef]
29. Luis, Z.G.; Bezerra, K.M.G.; Pereira, J.E.S. Adaptability and leaf anatomical features in oil palm seedlings produced by embryo rescue and pre-germinated seeds. *Plant Physiol.* **2010**, *22*, 209–215. [CrossRef]
30. Theocharis, A.; Clément, C.; Barka, E.A. Physiological and molecular changes in plants grown at low temperatures. *Planta* **2012**, *235*, 1091–1105. [CrossRef]
31. Kurbidaeva, A.S.; Novokreshchenova, M.G. Genetic control of plant resistance to cold. *Russ. J. Genet.* **2011**, *47*, 646–661. [CrossRef]
32. Fei, J.; Wang, Y.S.; Cheng, H.; Sun, F.L.; Sun, C.C. Comparative physiological and proteomic analyses of mangrove plant *Kandelia obovata* under cold stress. *Ecotoxicology* **2021**, *30*, 1826–1840. [CrossRef]
33. Peng, Y.L.; Wang, Y.S.; Fei, J.; Sun, C.C.; Cheng, H. Ecophysiological differences between three mangrove seedlings (*kandelia obovata*, *aegiceras corniculatum*, and *avicennia marina*) exposed to chilling stress. *Ecotoxicology* **2015**, *24*, 7–8. [CrossRef]
34. Provart, N.J.; Gil, P.; Chen, W.Q.; Han, B.; Chang, H.S.; Wang, X.; Zhu, T. Gene expression phenotypes of Arabidopsis associated with sensitivity to low temperatures. *Plant Physiol.* **2003**, *132*, 893–906. [CrossRef] [PubMed]
35. Liu, T.; Xu, J.J.; Li, J.M.; Hu, X.H. NO is involved in JA^{-} and $H_2O_2^{-}$ mediated ALA-induced oxidative stress tolerance at low temperatures in tomato. *Environ. Exp. Bot.* **2019**, *161*, 334–343. [CrossRef]
36. Orabi, S.A.; Dawood, M.G.; Salman, S.R. Comparative study between the physiological role of hydrogen peroxide and salicylic acid in alleviating the harmful effect of low temperature on tomato plants grown under sand-ponic culture. *Sci. Agric.* **2015**, *9*, 49–59.
37. Korn, M.; Peterek, S.; Mock, H.P.; Heyer, A.G.; Hincha, D.K. Heterosis in the freezing tolerance, and sugar and flavonoid contents of crosses between Arabidopsis thaliana accessions of widely varying freezing tolerance. *Plant. Cell Environ.* **2008**, *31*, 813–827. [CrossRef]
38. Schulz, E.; Tohge, T.; Zuther, E.; Fernie, A.R.; Hincha, D.K. Natural variation in flavonol and anthocyanin metabolism during cold acclima-tion in Arabidopsis thaliana accessions. *Plant Cell Environ.* **2015**, *38*, 1658–1672. [CrossRef]